Mon. Not. R. Astron. Soc. **370,** 1213–1222 (2006) doi:10.1111/j.1365-2966.2006.10538.x

Central stellar populations of early-type galaxies in low-density environments

Maela Collobert,[1⋆] Marc Sarzi,[1,2] Roger L. Davies,[1] Harald Kuntschner[3] and Matthew Colless[4]

[1]*University of Oxford, Astrophysics, Denys Wilkinson Building, Keble Road, Oxford OX1 3RH*
[2]*Centre for Astrophysics Research, University of Hertfordshire, College Lane, Hatfield, Herts AL10 9AB*
[3]*Space Telescope European Coordinating Facility, ESO, Karl-Schwarzschild-Str. 2, 85748 Garching, Germany*
[4]*Anglo-Australian Observatory, PO Box 296, Epping, NSW 2111, Australia*

Accepted 2006 May 5. Received 2006 May 1; in original form 2005 October 12

ABSTRACT

Following the pilot study of Kuntschner et al., we have investigated the properties of a volume- and magnitude-limited ($cz < 10\,000\,\mathrm{km\,s^{-1}}$, $b_J < 16$) sample of early-type galaxies that were carefully selected from the Anglo-Australian Observatory (AAO) two-degree field galaxy redshift survey (2dFGRS) to have no more than one and five companions within 1 and 2 Mpc, respectively. We used images from the Digital Sky Survey (DSS) to confirm the E/S0 morphologies. We augmented this sample with field galaxies from Colbert et al. selected as having no neighbour within 1 Mpc and $\pm 1000\,\mathrm{km\,s^{-1}}$. We present spectroscopic observations of 22 galaxies from the combined sample, from which central velocity dispersions and the Lick stellar population indices were measured. After carefully correcting the spectra for nebular emission, we derived luminosity-weighted ages, metallicities and α-element abundance ratios. We compare these isolated galaxies with samples of early-type galaxies in the Virgo and Coma clusters, and also with the previous sample of galaxies in low-density regions of Kuntschner et al. We find that galaxies in low-density environments are younger and have a greater spread of ages compared to cluster galaxies. They also show a wider range of metallicities at a given velocity dispersion than cluster galaxies, which display only supersolar metallicities. On average cluster, as well as, isolated galaxies show non-solar abundance ratios in α elements, suggesting that, independent of galactic environment, star formation occurred on short timescales. However, the abundance ratios for our low-density environment sample galaxies do not scale with the stellar velocity dispersion as observed in clusters. In fact we detect a large spread at a given velocity dispersion even reaching solar abundance ratios. The metallicity of isolated early-type galaxies is found to correlate weakly with σ. We reason that early-type galaxies in low-density environments experienced merging-induced star formation episodes over a longer and more recent period of time compared to a cluster environment, and speculate that a considerable fraction of their stars formed out of low-metallicity halo gaseous material during the slow growth of a stellar disc between merging events.

Key words: galaxies: abundances – galaxies: elliptical and lenticular, cD – galaxies: evolution – galaxies: formation.

1 INTRODUCTION

Understanding the formation and evolution of early-type galaxies is one of the major challenges for current structure–formation models. In particular, one key issue to be addressed is whether the environmental impact on the formation and evolution of galaxies predicted by N-body and semi-analytical models (e.g. Baugh, Cole & Frenk 1996; Kauffmann et al. 1999; Springel et al. 2001; Khochfar & Burkert 2003) is observed in real galaxies. In the framework of a cold dark matter (CDM) universe, structure assembles hierarchically by successive mergers of smaller structures. Observations of the galaxy merging rate in different environments suggest that interactions in high-density environments were more frequent than

⋆E-mail: maelasc@astro.ox.ac.uk

interactions in the field at high redshifts. Conversely interaction rates in the field are higher at low redshifts (van Dokkum et al. 1999; Le Fèvre et al. 2000). These trends are predicted by the CDM paradigm (e.g. Governato et al. 1999; Gottlöber, Klypin & Kravtsov 2001; Khochfar & Burkert 2001). For instance, in high-density environments rich clusters form quickly and subsequent merging between galaxies are suppressed by the large relative velocities. On the other hand, in low-density environments galaxies are still assembling today. The details of these predictions depend on a number of parameters, such as active galactic nucleus (AGN) or supernovae feedback processes, gas cooling and accretion rates and, particularly in clusters, tidal interactions and ram-pressure gas stripping.

In order to constrain the models it is crucial to study galaxies in *both* high- and low-density environments. In particular, we need to measure the age, metallicity and α-element abundance ratio of their main stellar constituents. However, the stellar population properties of elliptical and lenticular galaxies in low-density environments have received little attention because of the difficulty in identifying a reasonable sample. Based on a sample of nine galaxies with less than two neighbours within $\sim$1.3 Mpc, Kuntschner et al. (2002, hereafter K02) found that galaxies in low-density environments are on average younger, have higher metallicity and exhibit gas emission more frequently than similar galaxies in the Fornax cluster. The presence of young stellar populations could explain why isolated galaxies seem to fall below the fundamental plane and have lower mass-to-light ratios (Reda, Forbes & Hau 2005).

Following the pilot study of K02, we set out to identify a larger sample of early-type galaxies in low-density regions and to study their stellar populations. We compute the Lick indices and look for correlations with the velocity dispersion. We correct the absorption indices, in particular the Balmer indices, for the biases introduced by the presence of emission, using the emission-line removal method of Sarzi et al. (2006). We use the single stellar population (SSP) models of Thomas, Maraston & Bender (2003a, hereafter TMB03) to derive ages, metallicities and α-abundance ratios for our sample galaxies.

This paper is organized as follows. In Section 2, we describe the selection of our sample. In Section 3, we present the observations and the basic data reduction, along with the methods used to measure the galaxy recession velocity, central velocity dispersion, emission-line fluxes and Lick absorption-line indices. In Section 4, we compare different index combinations with SSP models to derive the luminosity-weighted mean stellar age, metallicity and abundance ratio of our sample galaxies. Finally, in Section 5, we discuss our results and draw our conclusions.

2 SAMPLE SELECTION

Our sample consists of two subsamples. The first include galaxies in low-density environment that were selected using the Anglo-Australian Observatory (AAO) two-degree field galaxy redshift survey (2dFGRS; Colless et al. 2001) and the other is drawn from the sample of isolated galaxies of Colbert, Mulchaey & Zabludoff (2001). The galaxies from the 2dFGRS survey were carefully chosen using well-defined criteria. We first selected galaxies with recession velocity $cz < 10\,000\,\mathrm{km\,s^{-1}}$ and apparent magnitude $b_J < 16$, corresponding to a limiting absolute magnitude of $M_B \leqslant -19.13$. This resulted in a volume- and magnitude-limited sample of 443 candidate galaxies. For each candidate, we then determined the number of companion galaxies within a sphere of radius 1 and 2 Mpc h^{-1} at least as bright as the candidate. When no velocity was available for a companion, we assumed it was at the same distance as the candidate. In this way we are conservatively overestimating the number of nearby companions. We selected only candidate galaxies with no more than one and five companions within 1 and 2 Mpc^{-1}, respectively, leaving around 200 candidates. We further restricted the number of candidates by keeping only objects with 2dFGRS spectra of sufficient quality to confidently exclude the presence of strong emission lines. We checked the morphology of these candidates with the Digital Sky Survey (DSS) and NASA/IPAC Extragalactic Database (NED) and eliminated those with obvious spiral or disturbed morphologies, ending up with about 30 galaxies. Of these, we observed 11 galaxies from the Siding Spring Observatory in Australia (see also Section 3.1). The morphology of the 2dFGRS targets was further checked a posteriori using images from the 2 Micron All Sky Survey (2MASS), which are shown in Fig. 1.

We added to this sample of galaxies in low-density environments, 11 isolated galaxies taken from the sample of Colbert et al. (2001). They were selected as isolated objects from the Third Reference Catalogue of Bright Galaxies (RC3) with no cataloged galaxies with known redshift within a projected radius of 1 Mpc h^{-1} and a velocity of $\pm 1000\,\mathrm{km\,s^{-1}}$. Furthermore, a maximum recession velocity of $cz = 10\,000\,\mathrm{km\,s^{-1}}$ was imposed.

Table 1 lists the observed sample galaxies, along with their main characteristics. We note that the Hubble classification for the galaxies in our 2dFGRS subsample should be considered with care, as

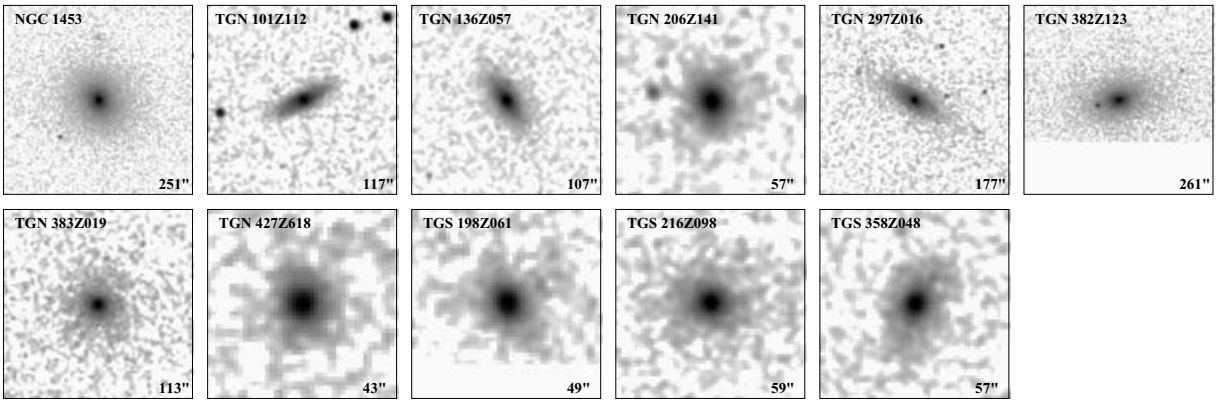

Figure 1. 2MASS 'postage stamp' J-band images for the 11 galaxies of the 2dFGRS sample. In each panel the size of the image is indicated in arcsec in the lower right, and north is up and east is left.

Table 1. Observed galaxies in low-density environments: 2dFGRS and Colbert et al. (2001) sample, and calibration Lick galaxies.

Name (1)	RA (B1950) (2)	Dec. (B1950) (3)	b_J (4)	Type (5)	cz (6)	σ (7)	Run (8)
			2dFGRS sample				
NGC 1453	$3^h43^m57\overset{s}{.}4$	$-4°07'24''$	12.77	E2-3	3934± 9	314 ± 10	2000 Dec
TGN 101Z112	$10^h36^m36\overset{s}{.}5$	$-5°14'29''$	15.03	S0	8330 ± 11	241 ± 11	2001 Apr
TGN 136Z057	$13^h22^m18\overset{s}{.}0$	$-3°49'24''$	14.44	S0	6132 ± 18	353 ± 17	2001 Apr
TGN 206Z141	$14^h08^m06\overset{s}{.}0$	$-2°26'57''$	15.50	E	8093 ± 8	166 ± 9	2001 Apr
TGN 297Z016	$10^h49^m33\overset{s}{.}6$	$-0°17'47''$	14.51	S0/a	5515 ± 9	138 ± 12	2001 Apr
TGN 382Z123	$12^h01^m54\overset{s}{.}0$	$+2°10'22''$	14.36	E	5871 ± 11	302 ± 11	2001 Apr
TGN 383Z019	$12^h08^m31\overset{s}{.}0$	$+1°15'06''$	14.21	S0−	6092 ± 10	130 ± 14	2001 Apr
TGN 427Z618	$10^h32^m16\overset{s}{.}0$	$+0°56'06''$	15.71	E	9502 ± 11	111 ± 17	2001 Apr
TGS 198Z061	$23^h59^m01\overset{s}{.}5$	$-27°51'08''$	15.36	E	8021 ± 22	148 ± 24	2000 Dec
TGS 216Z098	$1^h22^m49\overset{s}{.}6$	$-27°30'24''$	15.14	E	9330 ± 10	214 ± 13	2000 Dec
TGS 358Z048	$0^h02^m58\overset{s}{.}2$	$-30°51'55''$	15.37	S0	8330 ± 11	132 ± 11	2000 Dec
			Galaxies from Colbert et al. (2001)				
A0718−34	$7^h18^m56\overset{s}{.}2$	$-34°01'25''$	15.8	SA0−	8500 ± 15	256 ± 19	2000 Dec
ESO 065−G001	$12^h34^m05\overset{s}{.}0$	$-72°18'53''$	14.50	E4	7099 ± 15	236 ± 18	2001 Apr
ESO 505−G015	$12^h04^m33\overset{s}{.}0$	$-25°24'53''$	14.55	E+3	7451 ± 10	284 ± 11	2001 Apr
ESO 574−G017	$12^h37^m58\overset{s}{.}0$	$-20°17'15''$	15.22	E+	8428 ± 10	156 ± 13	2001 Apr
IC 1156	$15^h58^m25\overset{s}{.}0$	$+19°51'44''$	14.48	E	9213 ± 9	234 ± 11	2001 Apr
IC 2980	$11^h54^m59\overset{s}{.}9$	$-73°24'24''$	14.6	E3	2092 ± 6	141 ± 8	2000 Dec
IIZW017	$4^h32^m42\overset{s}{.}0$	$-1°50'00''$	15.6	cE pec	9728 ± 8	143 ± 9	2000 Dec
NGC 179	$0^h35^m15\overset{s}{.}9$	$-18°07'27''$	14.30	SAB0−	5976 ± 9	260 ± 9	2000 Dec
NGC 1132	$2^h50^m19\overset{s}{.}6$	$-1°28'45''$	13.25	E	6935 ± 11	253 ± 13	2000 Dec
NGC 3332	$10^h37^m51\overset{s}{.}0$	$+9°26'40''$	13.34	(R)SA0−	5758 ± 7	226 ± 9	2000 Dec
NGC 6799	$19^h28^m11\overset{s}{.}0$	$-56°00'53''$	13.39	SA0−	3363 ± 6	157 ± 8	2001 Apr
			Lick galaxies				
NGC 1600	$4^h29^m11\overset{s}{.}7$	$-5°11'38''$	11.93	E3	4681 ± 8	315 ± 8	2000 Dec
NGC 1700	$4^h54^m28\overset{s}{.}6$	$-4°56'33''$	12.20	E4	3889 ± 7	246 ± 7	2000 Dec

Notes: column (1) lists the name of the galaxy; columns (2) and (3) list the B1950 coordinates; column (4) shows the (total) b_J magnitude; column (5) lists the type of the galaxy as found in NED or the SDSS; columns (6) and (7) list the recession velocity and the velocity dispersion, respectively, as measured from our spectra; column (8) indicates in which run the galaxy was observed.

it is based on photographic plates which makes it difficult to differentiate between lenticular and elliptical galaxies. Although the isolation criterion applied to select our 2dFGRS galaxies is less stringent than the one used by Colbert et al. (2001), for simplicity we refer hereafter to our sample galaxies as isolated, to distinguish it from the low-density environment sample of K02.

3 OBSERVATION AND DATA REDUCTION

3.1 Observational techniques

The spectra were obtained at the Australian National University (ANU) 2.3-m telescope at the Siding Spring Observatory, Australia, in two runs: 2000 December and 2001 April. The first run was entirely clear whereas in the second run we got only three nights of data. In both runs we used the Double Beam Spectrograph (Rodgers, Conroy & Bloxham 1988), the same instrument as K02. Our analysis is based on data from the blue arm. The spectra obtained with the red arm, which covers the 8100–9050 Å wavelength region, were not used. The details of the setup are given in Table 2.

The seeing was in the range ≈1.3–2.0 arcsec. A typical exposure time for galaxies was 3600 s, subdivided in multiple exposures bracketed by neon–argon lamp calibration spectra, for wavelength calibration. Spectrophotometric standard stars were also observed to calibrate the response function of the system. For comparison purposes, we observed two galaxies from the Lick sample, they are listed in Table 1. For the brighter galaxies, such as those from the Lick samples just one exposure was taken. The resulting rest-wavelength range is 3690–5600 Å, covering a range of Balmer and

Table 2. The instrumental setup.

Telescope	MSSSO (2.3 m)
Dates	2000 Dec 16–20, 2001 Apr 26–May 1
Instrument	DBS spectrograph (blue arm)
Spectral range	3690–5600 Å
Grating	600 lines mm^{-1}
Dispersion	1.1 Å $pixel^{-1}$
Resolution	≈2.3 Å
Spatial scale	0.91 arcsec $pixel^{-1}$
Slit width	2.0 arcsec
Detector	SITe (1752 × 532 pixels; 15 × 15μm)
Gain	1.0 e− ADU^{-1}
Read-out-noise	5.5 e− (rms)
Typical seeing	1.5 arcsec

metallic absorption lines such as Hβ, Hγ, Mg b, Fe5270, Fe5335 and the [O II]λ3727 and [O III]$\lambda\lambda$4959, 5007 emission lines.

3.2 Basic data reduction

The data reduction used standard IRAF software packages. Each frame was overscan corrected and bias subtracted. Both skyflats and domeflats were used to correct for the pixel-to-pixel sensitivity variations and illumination correction along the slit. The cosmic rays were removed using the algorithm of van Dokkum (2001), which rejects cosmic rays using a variation of Laplacian edge detection. The wavelength calibration was determined from the neon–argon lamp spectra.

One-dimensional spectra were extracted using the closest physical aperture size to the same equivalent circular aperture diameter used in K02, namely 1.08 kpc. This aperture will not subtend the same fraction of all our sample galaxies. Unfortunately not all our sample galaxies have measured effective radii R_e so that apertures with the same relative size could not be extracted. This drawback will not affect our conclusions, however. Using the Spectrographic Areal Unit for Research on Optical Nebulae (SAURON) integral-field spectrograph, Cappellari et al. (2006) and Kuntschner et al. (2006) have accurately estimated the effect of aperture corrections on the central velocity dispersion, the Hβ, Mg b and Fe5015 indices, after correcting them for gas emission. If we assume that the Fe5270 and Fe5335 indices are subject to similar aperture corrections as the Fe5015 index, even considering a quite conservative range of $0.1\,R_e$–$0.6\,R_e$ for the relative size of our 1.08-kpc aperture, the central velocity dispersion and indices we measured should not be subject to fluctuation larger than 10 per cent. This value is typically smaller or at most comparable to our error bars.

Finally, the relative continuum shape of our spectra was flux calibrated using the spectrophotometric standard star EG131 following Bacon et al. (2001) and Kuntschner et al. (2006), and multiple exposures of the same galaxies were co-added.

3.3 Central velocity dispersions and emission-line removal

In order to correct the line-strength indices for kinematical broadening and to account for emission-line contamination, we first measured the recession velocity V, and central velocity dispersions σ of our sample galaxies using the method of Cappellari & Emsellem (2004), and then applied the procedure described in Sarzi et al. (2006) to derive and remove the emission-line fluxes if emission was detected. The algorithm of Cappellari & Emsellem (2004) minimizes the impact of template mismatch on the derived stellar kinematics by combining a number of stellar templates to optimally match the galaxy spectra. We used templates from the new library of SSP models from Vazdekis (in preparation), which are based on a collection of around a thousand stellar spectra. The Vazdekis (1999) models are the base models of these new templates. The models range from 3500 to 7500 Å with a resolution of $\sim$2.3 Å. We used SSP models with ages between 1.00 and 17.78 Gyr and with metallicities of 0.2, 0, -0.38, -0.68, -1.28, -1.68. We extracted the stellar kinematics in the wavelength range from 4700 to 5600 Å, while masking the regions potentially affected by Hβ and [O III] emission. Emission from the N [O I]$\lambda\lambda$5198, 5200 doublet was never detected.

Once the stellar kinematics is constrained we removed the mask in the Hβ and [O III] regions and, following the approach of Sarzi et al. (2006), fit simultaneously the stellar spectrum and the Hβ and [O III] emission lines. This is done by adding a set of Gaussian templates representing the emission lines to the SSP models library, and by solving only for the position, width and amplitudes of the emission-line templates and the contribution of each SSP template. The latter are convolved by the stellar line-of-sight velocity distribution (LOSVD) previously derived. To minimize the impact of template mismatch in the Hβ region, we imposed on the Hβ lines the same kinematics as the [O III] doublet, which was derived in a first emission-line fit. We then measured the standard deviation in the residuals of our fit and deemed detected only emission lines with Gaussian amplitudes at least four times larger than the noise. Out of the 22 galaxies in our sample, Hβ and/or [O III] emission was detected in seven galaxies. We subtracted the detected Hβ and [O III] lines from the spectra, to produce 'emission-line free' data for the line-strength analysis.

We note that the relative strength of the Hβ to [O III] lines spanned a wide range of values, from zero to Hβ/[O III] $\geqslant$2. This suggests that when possible it is better not to rely on fixed Hβ/[O III] ratios, such as the Hβ/[O III] = 0.6 values proposed by Trager et al. (1998), to correct the Hβ absorption index.

We applied the same velocity dispersion and emission-line correction also to the spectra of K02, in order to have all low-density sample galaxies reduced in the same way.

3.4 Line-strength indices

We measured the Lick/image dissector scanner (IDS) indices as defined in Worthey & Ottaviani (1997) and Trager et al. (1998). As our data have higher spectral resolution than the spectra used by the Lick group, we needed to degrade our spectra in order to measure the indices, recognizing that we may loose information. We broadened the spectra with a Gaussian of wavelength-dependent width as the IDS resolution depended on wavelength. We then corrected the indices for velocity broadening using the method of Kuntschner (2000) using templates stars and the values for σ derived in the previous section. These two steps are needed before comparing our indices with the stellar population models. We did not apply any offset to our indices, since in general the typical offsets are relatively small (e.g. Norris, Sharples & Kuntschner 2006) and the index values measured for the two galaxies from the Lick sample that we observed were very similar to the published values. We measured the age-sensitive Balmer indices Hβ, and metallicity-sensitive indices Mg b, Fe5270, Fe5335 among others. The errors associated to the line-strength indices are obtained by Monte Carlo simulations, accounting for the statistical fluctuations in the spectra and for the uncertainties in the derived recession velocity and therefore on the position of the line and pseudo-continuum passbands. The indices and their errors, including CN_1, CN_2 and Ca4227, are given in Table 3. Recently Kuntschner (2004) found that Hβ is also sensitive to both the h_3 and h_4 higher moments of the LOSVD, while the Fe5070, Fe5335, Mg b indices are sensitive to h_4 only. For old stellar populations and $\sigma = 250\,\mathrm{km\,s^{-1}}$, h_4 values of ±0.1 can introduce variations as high as 15–20 per cent in the ages and metallicities of old stellar populations, respectively.

We also measured the h_3 and h_4 moments of the central LOSVD and found that in none of the sample galaxies the values for h_3 and h_4 were significant enough to modify the indices (in average $h_3 = -0.02 \pm 0.03$ and $h_4 = 0.02 \pm 0.04$).

4 RESULTS

In this section, we first analyse index versus central velocity dispersion measurements for the $\langle$Fe$\rangle$, Mg b and Hβ Lick/IDS indices. Then, using the TMB03 models, we investigate the luminosity-weighted mean age, metallicity and [α/Fe] ratios of the stellar

Table 3. Lick/IDS indices and derived stellar population parameters for the low-density environment galaxies.

Galaxy	Age (Gyr)	[Z/H]	[α/Fe]	CN_1 (mag)	CN_2 (mag)	Ca4227 (Å)	G4300 (Å)	Fe4383 (Å)	Hβ (Å)	Fe5015 (Å)	Mgb (Å)	Fe5270 (Å)	Fe5335 (Å)
NGC 1453	6.0	0.43	0.20	0.116	0.156	0.92	5.96	5.90	1.55	5.33	4.83	3.24	2.81
±	2.8	0.10	0.04	0.003	0.004	0.14	0.11	0.31	0.13	0.76	0.14	0.17	0.41
TGN 101Z112	15.0	0.17	0.15	0.094	0.136	1.18	6.66	6.34	1.49	5.41	4.40	3.20	2.31
±	1.9	0.08	0.06	0.006	0.007	0.17	0.20	0.43	0.17	0.86	0.23	0.27	0.52
TGN 136Z057	4.0	0.43	0.25	0.122	0.163	2.25	5.77	4.93	1.68	5.34	4.91	2.99	3.42
±	2.4	0.13	0.05	0.004	0.005	0.20	0.16	0.41	0.17	1.01	0.27	0.25	0.66

Notes: the full table is available in the electronic version of MNRAS.

populations. Finally, we explore the relations between these three parameters and the galaxy mass, as traced by σ.

4.1 Lick/IDS indices as function of velocity dispersion

Burstein et al. (1988), Jørgensen (1997) and Trager et al. (1998) showed that the Mg_2 and Hβ indices vary systematically with the velocity dispersion of galaxies σ, whereas the $\langle$Fe$\rangle$ index presents a rather weak correlation with σ (see also Kuntschner et al. 2001). We explored the correlation between line strength and the velocity dispersion, considering log $\langle$Fe$\rangle$ versus σ, Mg b' versus σ and Hβ' versus σ. The prime sign [$'$] is the index expressed in magnitudes like the 'molecular' indices (see e.g. Kuntschner et al. 2001).

Fig. 2 illustrates these relations for early-type galaxies from the high-density environment sample from Thomas et al. (2005, hereafter T05). This sample includes 11 galaxies from the Virgo cluster (González 1993), 32 from the Coma cluster (Mehlert et al. 2000, 2003) and 11 from Beuing et al. (2002). The latter objects were selected from the ESO-UV Catalog (Lauberts & Valentijn 1989) requiring a local galaxy surface density $NG_T > 9$ (NG_T being the number of galaxies per square degree inside a radius of 1° around the considered galaxy).

There is a good agreement between the relations shown in Fig. 2 and the literature (e.g. Colless et al. 1999; Kuntschner et al. 2001; Mehlert et al. 2003) for both the tight Mg–σ relation, and the anticorrelation between Hβ and σ. Few galaxies have velocity dispersions below $\sigma = 150\,\mathrm{km\,s^{-1}}$. There is no clear distinction between the S0s and Es, except for the Hβ' versus σ relation, where at a given σ the S0s are offset from the Es by ≈0.01 dex towards higher values.

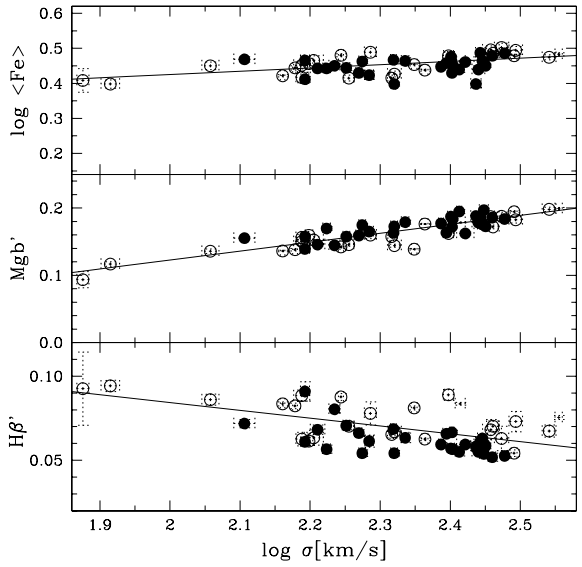

Figure 2. Relation between log ($\langle$Fe$\rangle$), Mg b', Hβ' and log σ for the cluster galaxies from T05. Open circles show the S0s, the filled circles represent the elliptical galaxies. The solid lines show a least-square fit to the data.

Fig. 3 shows the same diagrams for our sample on the left and for the low-density environments of K02 (hereafter, LDE) on the right. Besides the $\langle$Fe$\rangle$–σ relation of isolated galaxies being steeper than for the other two samples, the relations for the cluster, isolated and LDE samples have similar slopes within the uncertainties. The scatter in the relations derived for the isolated sample is however almost twice larger than in the case of the cluster or LDE samples. In detail, the rms for the log $\langle$Fe$\rangle$–log σ relation is 0.050 for the 2dFGRS/Colbert's sample, whereas it is only 0.023 and 0.035 for the cluster and LDE sample, respectively. Similarly, for the Mg b'–log σ relation it is 0.017 for the 2dFGRS/Colbert's sample, compared to a rms of 0.010 for the cluster environment and a rms of 0.009 for the LDE sample. Finally, for the Hβ'–log σ relation, we find a rms of 0.012, 0.009 and 0.008 for the 2dFGRS/Colbert's, the cluster and the LDE samples, respectively.

We note the distinct grouping in the velocity dispersion distribution of our sample with one group clustered around $150\,\mathrm{km\,s^{-1}}$ and another around $250\,\mathrm{km\,s^{-1}}$. This separation may be an artifact of our sample selection. No such dichotomy is present in our absolute magnitude distribution. Relatively more galaxies in our sample have a low velocity dispersion ($\log\sigma \leqslant 2.2$) than the cluster galaxies.

In summary, the relations between line-strength index and central velocity dispersion are on average quite similar for cluster galaxies and both samples of galaxies in low-density environments, following the same trends: negative correlation between Hβ and the velocity dispersion, increasing metal line strength (Mg b, $\langle$Fe$\rangle$) with increasing σ. However, we find a larger scatter for the early-type galaxies in low-density environments. Similarly, Denicolo et al. (2005a) found no significant differences in the index–σ relations between cluster and low-density region galaxies, except for a larger scatter for the group, field and isolated galaxies compared to the cluster galaxies.

4.2 Hβ versus [MgFe]$'$

In this section, we aim to derive robust and first-order estimates of the luminosity-weighted age and metallicity of our sample galaxies. A detailed investigation, including the abundance ratios, is presented in Section 4.4. The luminosity-weighed age of a population can be inferred from a comparison of selected line-strength indices with models of SSPs such as those of TMB03. In our study, we use Hβ as age indicator because its age sensitivity is greater and it is less degenerate with metallicity, or abundance ratio variations, than the

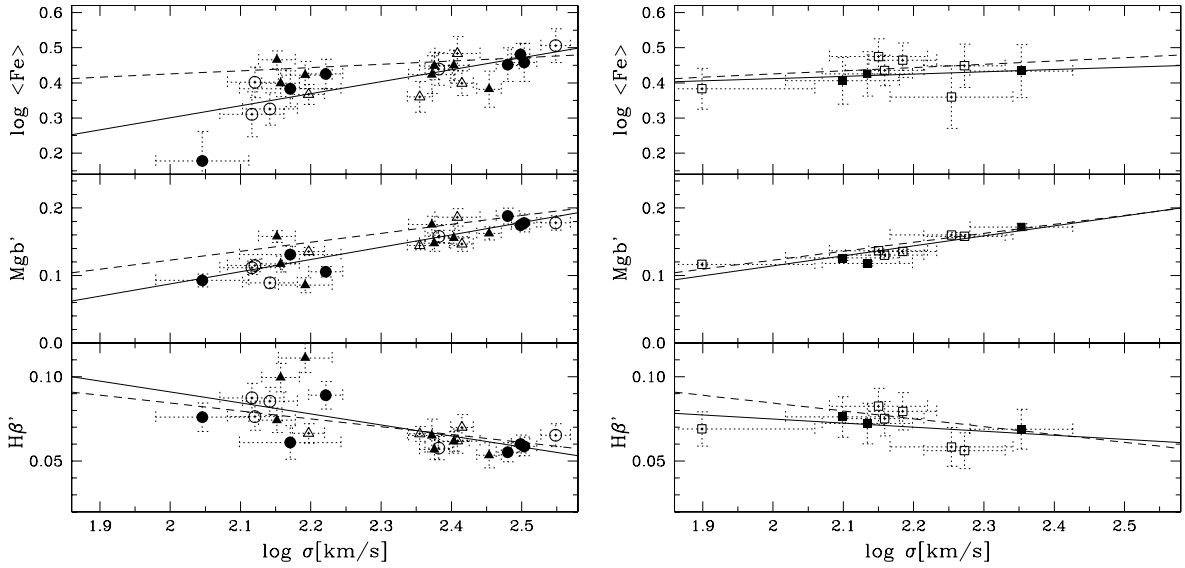

Figure 3. Relation between log (⟨Fe⟩), Mg b', Hβ' and log σ for the galaxies in low-density environments. In the left-hand plot, the 2dFGRS sample is represented by circles, Colbert's sample by triangles. The right-hand plot shows the K02 sample in rectangles. For both plots, the S0 galaxies are shown with open symbols, the ellipticals with filled symbols. In all panels the linear fit to the the data is shown by the solid line, whereas the dashed line shows for comparison the same fit for the cluster sample (see Fig. 2).

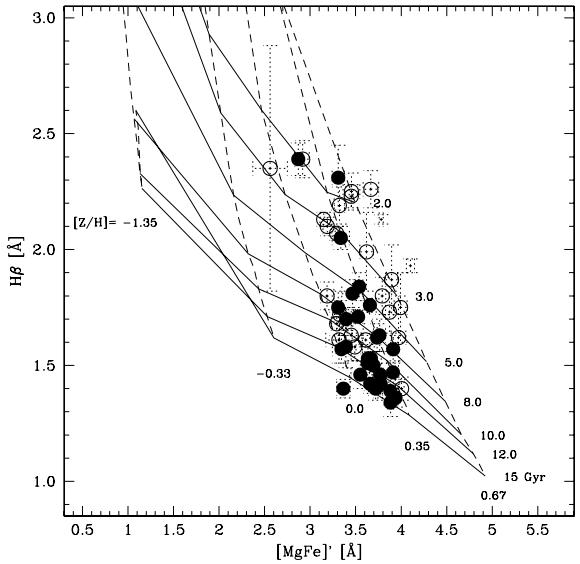

Figure 4. The age-sensitive index Hβ as a function of the metallicity-sensitive index [MgFe]$'$. Overplotted are the stellar population models of TMB03. The solid lines are lines of constant age from 2 to 15 Gyr. The dashed, almost vertical, lines stand for constant metallicity from [Z/H] = −1.35 to 0.67 dex. The age and metallicity steps are indicated to the right and at the bottom of the model predictions. The symbol definitions are the same as in Fig. 2.

Hγ index (see e.g. Korn, Maraston & Thomas 2005). As a metallicity indicator we adopt the [MgFe]$'$ index of TMB03 as it is virtually independent of abundance ratio variations.

Fig. 4 shows the distribution in Hβ versus [MgFe]$'$ for the cluster galaxies and a grid from the stellar population models of TMB03. The almost vertical lines are of constant metallicity and range from −2.25 to 0.67 dex, whereas the solid lines represent the age from 1 to 15 Gyr. We note that cluster galaxies appear to have a quite small range in metallicity for galaxies older than 5 Gyr; they are almost all between [Z/H] = 0 and 0.35 dex. Most of these galaxies are ellipticals. On the other hand, the younger galaxies, mainly S0s, have a larger spread in metallicity reaching [Z/H] = 0.67 dex.

Fig. 5 presents the same age–metallicity diagnostic plot but for the samples of field galaxies: on the left-hand panel, our sample of isolated galaxies and on the right-hand panel, the LDE sample of K02. Our isolated sample shows a wider spread in ages and metallicities than in the case of cluster galaxies. Most of our sample galaxies have ages between 3 and 15 Gyr and metallicities between −0.3 and 0.3. The LDE sample of K02 shows also a similar range of ages and metallicities. Our data is consistent with the low-density region galaxies of Denicolo et al. (2005b, hereafter D05b), which also show a large spread in age and metallicity. Taking the isolated and LDE samples together and considering the uncertainties in the Hubble classification of our sample, we do not find a clear relation between galaxy type and age or metallicity. On the other hand, early-type galaxies in clusters tend to have different properties depending on their type, S0s rather younger with a large range in metallicity and elliptical galaxies rather older with a small range in metallicity.

4.3 ⟨Fe⟩ versus Mg *b*

In this section, we have a first look at the abundance ratios of our sample galaxies. We investigate the Mg b versus ⟨Fe⟩ diagram (Figs 6 and 7), where the model prediction for solar abundance ratios spans a narrow region in parameter space. This diagram is a diagnostic for the star formation time-scale. Magnesium (like the other α elements) is formed in the explosion of Type II supernovae which occur rapidly after a burst of star formation whereas the iron peak elements originate in Type Ia supernovae which lag behind by at least 1 Gyr (Nomoto, Thielemann & Yokoi 1984; Woosley & Weaver 1995). Thus a supersolar α element to Fe ratio indicates that stars formed in an initial burst taking up the Type II supernova abundance pattern and then star formation ceased, perhaps through the onset of galactic winds sweeping away the gas material (Greggio &

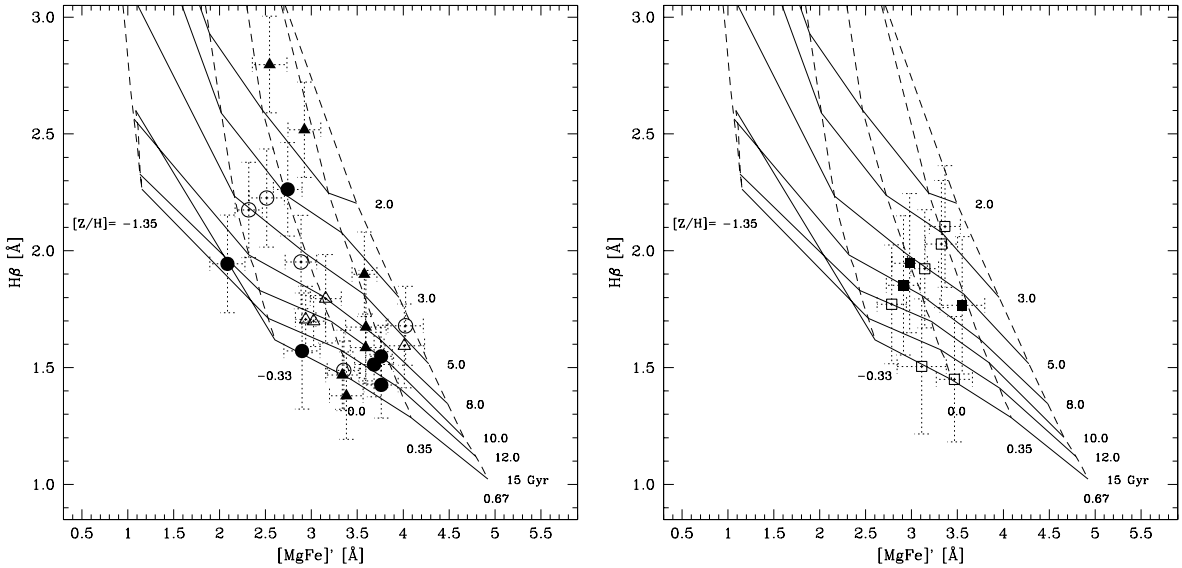

Figure 5. The Balmer-index Hβ as a function of [MgFe]$'$. The symbols are the same as Fig. 3. The left-hand plot shows the 2dFGRS and Colbert's sample, and the right-hand plot shows the LDE sample (K02).

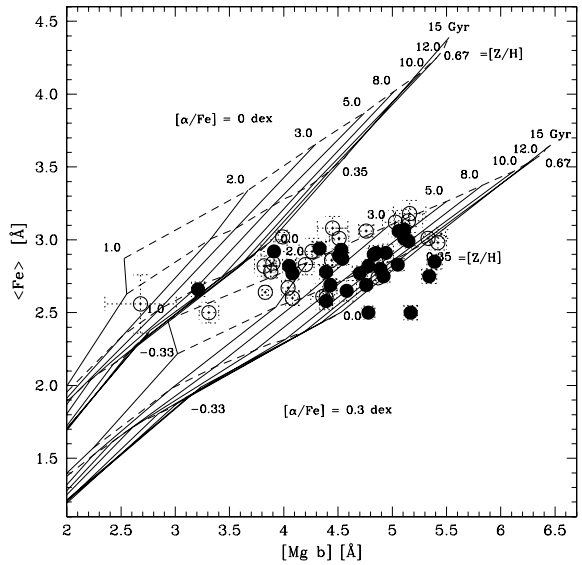

Figure 6. Mg b versus $\langle$Fe$\rangle$ for the cluster environments. Open and filled circles represent lenticular and elliptical galaxies, respectively. Overplotted are SSP models from TMB03 for solar and non-solar abundance ratios, [α/Fe] = 0.0 and 0.3 dex, respectively.

Renzini 1983; Matteucci & Greggio 1986; Thomas, Greggio & Bender 1998). These short star formation time-scales $\leqslant$1 Gyr are also interesting as they are not achieved by current models of hierarchical galaxy formation (e.g. Matteucci 1994; Thomas, Greggio & Bender 1999).

In Fig. 6, we plot galaxies in clusters. Most appear to have [α/Fe] ratios between 0 and 0.3 dex, and thus have on average clearly supersolar abundance ratios, a result first found by Worthey, Faber & González (1992). We note that the lenticular galaxies appear, in this diagram, to be closer to solar abundance ratios than the elliptical galaxies. However, this could be partly attributed to an age effect since the models are not completely degenerate in this parameter space (see Section 4.4 for a more rigorous analysis).

Fig. 7 shows the same distribution but for our sample (left-hand panel), and the LDE galaxies (right-hand panel). The plots are very similar, there is no obvious difference between ellipticals and S0s (in contrast to the clusters galaxies) or between our 2dFGRS/Colbert sample of isolated galaxies and the LDE sample of K02. Most isolated and LDE galaxies display a clear α enhancement, although at lower level than the cluster galaxies.

The Mg b versus $\langle$Fe$\rangle$ diagram can be used to obtain a first estimate of the abundance ratios but the result crucially depends on the age and metallicity assumed. Often these quantities are estimated using diagrams opposing two indices that are intended to be sensitive only to age and metallicity, such as the Hβ versus [MgFe]$'$ diagrams of Section 4.2. However, a perhaps more economic and precise way of deriving age, metallicity and abundance ratio estimates is the χ^2 fitting approach pioneered by Proctor, Forbes & Beasley (2004, hereafter P04). We will explore this technique in the next section.

4.4 Determination of age, metallicity and abundance ratios

P04 pointed out that diagrams using only a few indices such as Hβ or Hγ versus [MgFe] (see e.g. González 1993) can lead to inconsistent age estimates, even when used to derive the age of globular clusters. In order to improve the stellar population analysis P04 proposed to solve (χ^2 minimization) for the best-fitting stellar population parameters using a large set of indices. This new method is making better use of the information on the age, metallicity and abundance ratio which is contained in all the indices rather than being biased by a few selected indices.

In our application of the method, we interpolated all tabulated indices from TMB03 in steps of 0.025 in metallicity, 0.05 in [α/Fe] and 1 Gyr in age. The actual χ^2 minimization was performed in the log age, [Z/H] and [α/Fe] parameter space. Among the indices we measured, we decided to use only G4300, Fe4383, Hβ, Fe5015, Mg b, Fe5270 and Fe5335 in the analysis. We excluded the CN_1, CN_2 and Ca4227 indices because they are not well reproduced within the TMB03 models (Tripicco & Bell 1995; Thomas, Maraston & Bender 2003b; P04). Errors on the final estimates were obtained

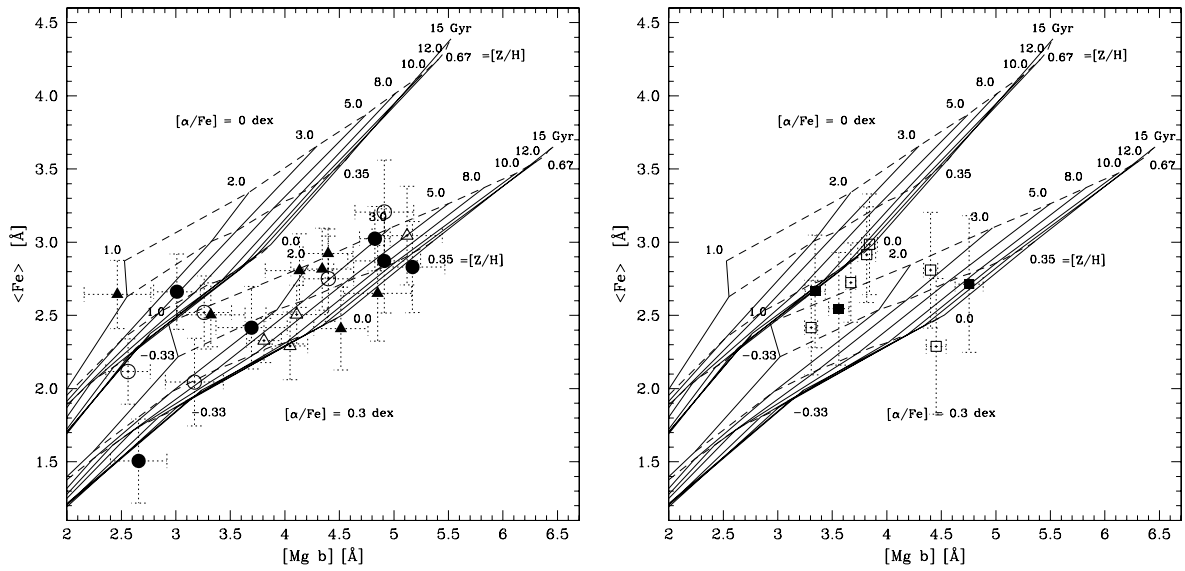

Figure 7. The index ⟨Fe⟩ as a function of Mg *b*, with stellar population models overplotted. These are the same as in Fig. 6. The symbols are the same as in Fig. 3.

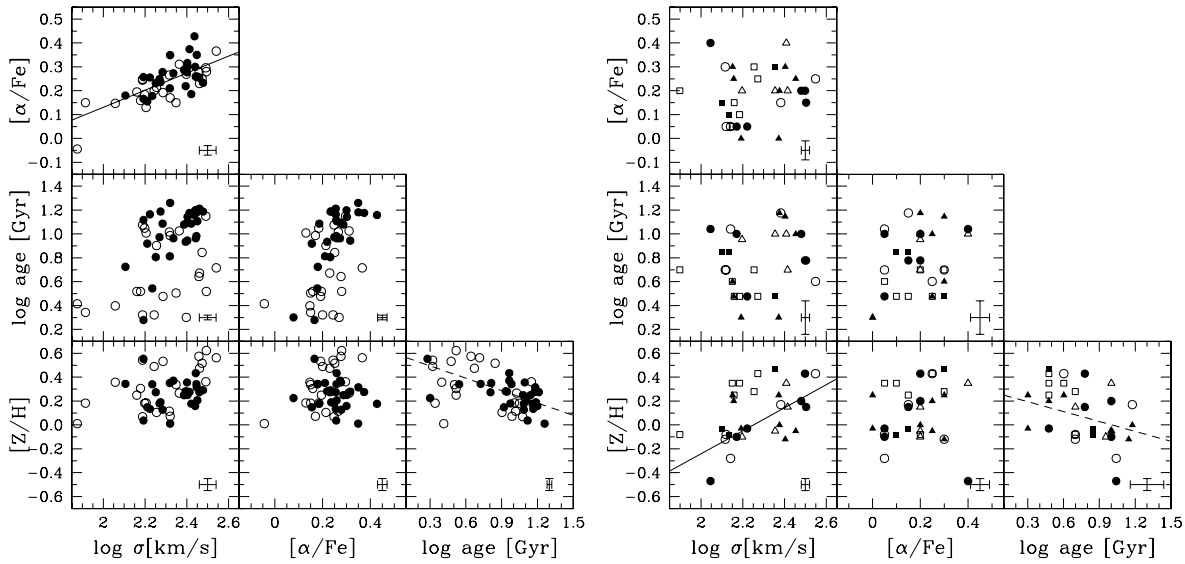

Figure 8. The global relations between log age, [Z/H], [α/Fe] and log σ are shown. The symbols are the same as in Figs 3 and 2. The left-hand plot shows the clusters galaxies, the right-hand panel combines the 2dFGRS and Colbert's samples with the LDE sample. The solid lines identify a least-square fit between the parameters. Typical error bars are shown at the lower-right corner of each diagram. These do not account for the fact that the errors on age, [Z/H] and [α/Fe] can be correlated, which can impact the significance of the observed correlations between these parameters. In particular, this can be the case for the age–[Z/H] relations, which are shown by dashed lines.

by Monte Carlo simulations using the errors on the index measurements.

The right-hand panel of Fig. 8 shows our final results for the isolated galaxies in our sample together with the galaxies in the LDE sample of K02, since these samples have very similar properties. The left-hand panel of Fig. 8 shows the same plots for the cluster galaxies of T05. A similar figure was presented by T05, but included only galaxies older than 5 Gyr, i.e. their old subsample. T05 obtained their values by first fixing the abundance ratio and determining the ages and metallicities with the two pairs (Hβ, Mg *b*) and (Hβ, ⟨Fe⟩), then used the metallicities found for Mg *b* and ⟨Fe⟩ to adjust the abundance ratio, and iterated until consistent results between both pairs were found. Table 3 gives our age, metallicity and abundance ratios estimates and associated errors for the low-density environment galaxy sample. The full table is available in the electronic version of MNRAS.

If we look first at galaxies in clusters (left-hand panel), we notice the clear correlation between [α/Fe] and log σ found also by e.g. Kuntschner (2000), Kuntschner et al. (2001) and T05. The three top plots show that old galaxies have also higher velocity dispersions and higher abundance ratios than younger objects. Similarly, Caldwell, Rose & Concannon (2003) and Trager et al. (2000) claim that there is a trend for lower σ elliptical galaxies to have younger ages. Using a Spearman rank–order test between σ and age, we find

that ellipticals follow a better trend of σ with age than S0s (98 per cent probability for the existence of a correlation for Es and 85 per cent probability for S0s) as on average the scatter for the S0s is larger. Furthermore, on average Es are older than S0s, with mean luminosity-weighted ages of 11 and 6 Gyr for Es and S0s, respectively. From the plots against the metallicity, the cluster galaxies appear to have only supersolar metallicities, with an average [Z/H] ≈ 0.27, and no clear trend with σ or abundance ratio. There also appears to be a weak anticorrelation between [Z/H] and age. Spearman rank–order tests yield a 60 and 95 per cent probability that a correlation exists for Es and S0s, respectively. However, the true significance of such a relation is difficult to assess, since the errors in age and metallicity are correlated in the direction of the potential relation (see e.g. Kuntschner et al. 2001; T05, for details). Correlations between σ and age, [Z/H] and [α/Fe] for cluster galaxies were also found by T05 (but see also references therein).

In contrast, for the isolated and LDE galaxies (right-hand panel), we notice in all the plots a large spread in age, metallicity and abundance ratio. A Spearman rank–order test suggests that metallicity is correlated with σ or age with a probability of 95 per cent, although as in the case of the cluster galaxies, the relation between metallicity and age would need to be confirmed.

We note that contrary to this study both K02 and T05 found evidence for slightly higher [Z/H] in field early-type galaxies than in clusters. The discrepancy with the results of T05 may be due to a different sample selection. Most of the field galaxies of T05 are not as 'isolated' as the ones in our and K02 samples. On the other hand, the difference between the conclusions on the stellar metallicity reached by us and K02 arise from (a) our use of a more accurate correction for the emission-line contamination, (b) re-analyzing the data of K02 with the latest SSP models and (c) from the fact that the cluster of reference in K02, Fornax, have different population properties than the Virgo and Coma clusters from T05 used here. In agreement with our work, Bernardi et al. (2006) and Smith et al. (2006) detect a statistically significant offset towards younger ages for galaxies in lower density regions as derived from large surveys (SDSS and NOAO Fundamental Plane Survey, respectively). The above mentioned investigations also find a small, but significant, offset in abundance ratio between different environments and no offset in metallicity. Given our small sample size and that their definition of environment is sufficiently different from ours, it is difficult to judge the degree of agreement between our results. However, we reemphasize here that our low-density environment sample shows a larger spread in age, metallicity and abundance ratio as compared to the cluster environment.

The large scatter we find for the luminosity-weighted ages of early-type galaxies in low-density environments is in agreement with the predictions of semi-analytical models (e.g. Cole et al. 2000; see also K02). Additionally, some of the early-type galaxies with velocity dispersions of about 150 km s^{-1} reach solar abundance ratios which would be expected in a hierarchical formation scenario with extended star formation episodes for galaxies in low-density regions (e.g. Thomas & Kauffmann 1999). However, we still find that the most massive galaxies (i.e. highest velocity dispersion) in the low-density environments show similar abundance ratios as cluster galaxies and thus have supersolar ratios which is difficult to explain in hierarchical formation scenarios. Similarly, puzzling is also the finding of supersolar abundance ratios in less massive galaxies, which was already noticed by D05b.

Finally, we note that ellipticals and S0s appear to be indistinguishable in low-density environments, which could reflect our inability to separate elliptical from lenticular galaxies on the basis of DSS images. On the other hand, only one third of the combined isolated and LDE samples were classified in this way and the majority of the objects have well-defined morphologies. Hence elliptical galaxies and S0s in low-density environments appear to have similar stellar populations, in contrast to what is observed in clusters.

Overall, galaxies in low-density environments exhibit a more uniform distribution of luminosity-weighted stellar age and a broader range in metallicity than their counterparts in clusters, and on average also appear to be younger. Galaxies in low-density environments can achieve the same degree of non-solar abundance ratios as galaxies in clusters, although a larger range of [α/Fe] ratios, even reaching solar values at intermediate velocity dispersions, is observed. The large range in stellar population parameters and lack of correlation with central velocity dispersion observed in our sample is indicative of a more diverse galaxy formation scenario in the field as compared to the typical cluster environment.

5 CONCLUSIONS

Following the pilot project of K02, we set out to study the stellar populations of a larger and more accurately selected sample of galaxies in low-density environments. We have used spectroscopic data from the 2dFGRS survey to select galaxies without strong Hα emission and with no more than one and five companion within 1 and 2 Mpc^{-1}, respectively, and combined these objects with isolated early-type galaxies from the sample of Colbert et al. (2001), which have no companions within 1 Mpc.

We measured a set of Lick/IDS indices to obtain estimates of the luminosity-weighted mean age, metallicity and abundance ratio in our sample galaxies. We also applied a new technique (Sarzi et al. 2006) to subtract gaseous emission from our spectra before measuring the absorption line-strength indices. The stellar population estimates were obtained with the models of TMB03 and the χ^2 technique of P04.

By applying the same methodology to the data of K02, we find that the stellar population properties of the galaxies of K02 appear to be very similar to that of our sample galaxies. After combining all low-density environment samples together (yielding a sample of 31 galaxies), we find that, compared to the cluster galaxies from the compilation of T05, early-type galaxies in low-density environments.

(i) Show a more uniform distribution of luminosity-weighted stellar ages ranging from $\sim$2 to 15 Gyr and thus have on average younger stellar populations. This is particularly true for elliptical galaxies.

(ii) Display a broader range of stellar metallicities, extending to subsolar values at similar central velocity dispersions, σ.

(iii) Can also reach the same amount of non-solar abundance ratios as cluster galaxies. However, there is an increased scatter at fixed σ with no clear correlation between [α/Fe] and σ.

(iv) Elliptical galaxies and S0s in low-density environments have stellar populations that are indistinguishable within our sample in contrast to the cluster galaxies, where there is a significant distinction between younger S0s and older elliptical galaxies.

How do these results compare with the predictions of galaxy formation models (e.g. Cole et al. 2000)? According to the models, galaxies in clusters assemble early, when they repeatedly experienced short star formation episodes each time they merged. More recently, however, galaxies in clusters do not merge owing to their high relative velocities. On the other hand, galaxies in the field

initially merge less often (e.g. Khochfar & Burkert 2001), while merging continues to low redshifts.

Hence, even considering only merging-induced star formation, early-type galaxies in low-density environments are expected to show a wider range of ages for their stellar constituents, compared to the stars in cluster galaxies. This is qualitatively consistent with our findings as also previously reported by K02 and T05.

In addition, the larger range of [α/Fe] and metallicities observed in field early-type galaxies suggest further differences between the evolutionary paths of cluster and field galaxies. The large range of [α/Fe] ratios reaching solar values indicates that at least some field galaxies experienced extended star formation episodes. We can speculate that these stars formed in the discs that grew between merger events (Khochfar & Silk 2006). Finally, we note that the ability of galaxies in low-density environments to grow stellar discs around them in recent epochs may explain why early-type galaxies in low-density environments are so scarce and very often show morphological signatures (such as outer shells or dusts; Colbert et al. 2001; K02) of recent merging events. In other words, most galaxies in the field that we classify as E or S0 may have assembled only recently.

ACKNOWLEDGMENTS

We wish to thank Sadegh Khochfar and Daniel Thomas for many helpful discussions.

REFERENCES

Bacon R. et al., 2001, MNRAS, 326, 23
Baugh C. M., Cole S., Frenk C. S., 1996, MNRAS, 283, 1361
Bernardi M., Nichol R. C., Sheth R. K., Miller C. J., Brinkmann J., 2006, AJ, 131, 1288
Beuing J., Bender R., Mendes de Oliviera C., Thomas D., Maraston C., 2002, A&A, 395, 431
Burstein D., Bertola F., Buson L. M., Faber S. M., Lauer T. R., 1988, ApJ, 328, 440
Caldwell N., Rose J. A., Concannon K. D., 2003, AJ, 125, 2891
Cappellari M., Emsellem E., 2004, PASP, 116, 138
Cappellari M. et al., 2006, MNRAS, 366, 1126
Colbert J. W., Mulchaey J. S., Zabludoff A. I., 2001, ApJ, 121, 808
Cole S., Lacey C. G., Baugh C. M., Frenk C. S., 2000, MNRAS, 319, 168
Colless M., Burstein D., Davies R. L., McMahan R. K., Saglia R. P., Wegner G., 1999, MNRAS, 303, 813
Colless M. et al., 2001, MNRAS, 328, 1039
Denicolo G., Terlevich R., Terlevich E., Forbes D. A., Terlevich A., Carrasco L., 2005a, MNRAS, 356, 1440
Denicolo G., Terlevich R., Terlevich E., Forbes D. A., Terlevich A., 2005b, MNRAS, 358, 813 (D05b)
González J. J., 1993, PhD thesis, Univ. California, Santa Cruz
Gottlöber S., Klypin A., Kravtsov A. V., 2001, ApJ, 546, 223
Governato F., Gardner J. P., Stadel J., Quinn T., Lake G., 1999, AJ, 117, 1651
Greggio L., Renzini A., 1983, A&A, 118, 217
Jørgensen I., 1997, MNRAS, 288, 161
Kauffmann G., Colberg J. M., Diaferio A., White S. D. M., 1999, MNRAS, 303, 188
Khochfar S., Burkert A., 2001, ApJ, 561, 517
Khochfar S., Burkert A., 2003, ApJ, 597, L117
Khochfar S., Silk J., 2006, MNRAS, in press (doi:10.1111/j.1365-2966.2006.10533.x) (astro-ph/0509375)
Korn A. J., Maraston C., Thomas D., 2005, A&A, 438, 685
Kuntschner H., 2000, MNRAS, 315, 184
Kuntschner H., 2004, A&A, 426, 737
Kuntschner H., Lucey J. R., Smith R. J., Hudson M. J., Davies R. L., 2001, MNRAS, 323, 615
Kuntschner H., Russell J. S., Colless M., Davies R. L., Kaldare R., Vazdekis A., 2002, MNRAS, 337, 172 (K02)
Kuntschner H. et al., 2006, MNRAS, 369, 497
Lauberts A., Valentijn E. A., 1989, The Surface Photometry Catalogue of the ESO–Upsalla Galaxies. ESO, Garching
Le Fèvre O. et al., 2000, MNRAS, 311, 565
Matteucci F., 1994, A&A, 288, 57
Matteucci F., Greggio L., 1986, A&A, 154, 279
Mehlert D., Saglia R. P., Bender R., Wegner G., 2000, A&AS, 141, 449
Mehlert D., Thomas D., Saglia R. P., Bender R., Wegner G., 2003, A&AS, 407, 423
Nomoto K., Thielemann F. K., Yokoi K., 1984, ApJ, 286, 644
Norris M. A., Sharples R. M., Kuntschner H., 2006, MNRAS, 367, 815
Proctor R. N., Forbes D. A., Beasley M. A., 2004, MNRAS, 355, 1327 (P04)
Reda F. M., Forbes D. A., Hau G. K. T., 2005, MNRAS, 360, 693
Rodgers A. W., Conroy P., Bloxham G., 1988, PASP, 100, 626
Sarzi M. et al., 2006, MNRAS, 366, 1151
Smith R. J., Hudson M. J., Lucey J. R., Nelan J. E., Wegner G. A., 2006, MNRAS, submitted (astro-ph/0603588)
Springel V., White S. D. M., Tormen G., Kauffmann G., 2001, MNRAS, 328, 726
Thomas D., Kauffmann G., 1999, ASP Conf. Ser. Vol. 192, Spectrophotometric Dating of Stars and Galaxies. Astron. Soc. Pac., San Francisco, p. 261
Thomas D., Greggio L., Bender R., 1998, MNRAS, 296, 119
Thomas D., Greggio L., Bender R., 1999, MNRAS, 302, 537
Thomas D., Maraston C., Bender R., 2003a, MNRAS, 339, 897 (TMB03)
Thomas D., Maraston C., Bender R., 2003b, MNRAS, 343, 279
Thomas D., Maraston C., Bender R., de Oliveira C. M., 2005, ApJ, 621, 673 (T05)
Trager S. C., Worthey G., Faber S. M., Burstein D., González J. J., 1998, ApJS, 116, 1
Trager S. C., Faber S. M., Worthey G., González J. J., 2000, AJ, 120, 165
Tripicco M. J., Bell R. A., 1995, AJ, 110, 3035
van Dokkum P. G., 2001, PASP, 113, 1420
van Dokkum P. G., Franx M., Fabricant D., Kelson D. D., Illingworth G. D., 1999, ApJ, 520, L95
Vazdekis A., 1999, ApJ, 513, 224
Woosley S. E., Weaver T. A., 1995, ApJS, 101, 181
Worthey G., Ottaviani D. L., 1997, ApJS, 111, 377
Worthey G., Faber S. M., González J. J., 1992, ApJ, 398, 69

This paper has been typeset from a TEX/LATEX file prepared by the author.